

# Investigating the Impact of Annealing and Thickness on the Optical and Electrical Characteristics of ZnO (TCO) for Optoelectronics Devices

Shruti Bakshi and Suman Rani\*

Department of Physics, School of Chemical Engineering & Physical Sciences, Lovely Professional University, Punjab-144411, India

Received: 31 Jul. 2024, Revised: 24 Feb. 2025, Accepted: 24 Feb. 2025

Published online: 1 May 2025

**Abstract:** In this paper, we investigate Transparent Conducting Oxides (TCO) thin films, which have created immense interest in researchers due to their widespread utilization in optoelectronics devices. Annealing and thickness are two main characteristics of thin films that influence the optical and electrical properties of the ZnO thin films in terms of band gap energy. The goal of the study is to analyze the influence of annealing and thickness of thin films on the optical and electrical properties of zinc oxide thin films. The ZnO thin films were prepared with different layers, and annealing temperatures were at 300°C, 400°C and 500°C. In XRD analysis, ZnO thin films exhibit a hexagonal crystal structure and reveal that crystallite size increases with the increase of annealing temperature. The transmission is strongly influenced by annealing temperature and thickness. At 500°C and thickness 189nm, 83% transmission is achieved in the visible region. The conductivity and activation energy of the ZnO thin film increases with the increase of annealing temperature and decreases with the increase of thickness. At 500°C and 189nm thickness, the value of conductivity and activation energy is  $1.02 \times 10^4 (\text{Scm}^{-1})$  and  $E_{a1}=0.570\text{eV}$ ,  $E_{a2}=0.865\text{eV}$ . The Figure of merit suggests that ZnO thin film will behave better at 500°C with 189nm among six deposition layers supporting its use as an affordable transparent conducting oxide thin film in optoelectronics devices.

**Keywords:** ZnO thin films, Transmission, Conductivity, Transparent Conducting Oxides, Optoelectronics devices, Solar cells.

## 1. Introduction

Over the past few decades, Transparent Conducting Oxides (TCO) thin films have created immense interest in researchers due to their widespread utilization in optoelectronics devices such as touch screens, liquid crystal displays, Light Emitting Diodes (LED), and solar cells [1-3]. Transparent Conducting Oxides (TCO) show the properties of high transmission and high electrical conductivity in the spectrum of visible region (380-700nm). Due to its excellent electrical conductivity and high transmission to visible light, Indium tin Oxide (ITO) is the most widely utilized transparent conducting oxide material [4]. However, there is crucial research in finding a suitable alternative material for ITO due to its huge price, toxicity, and scarcity of indium as it is the main component element [5]. In this concern, ZnO material has emerged as a promising candidate in place of ITO due to its lower price, non-toxicity, and thermal and chemical stability [6]. Cost-effectiveness and non-toxicity are crucial components in the part of the practical field [7]. ZnO thin film has tremendous applications in the fields of optoelectronics, electronics, corrosion protection, pharmaceutical industries,

and chemical industry [8]. The optical transparency and electrical properties are greatly affected by the thickness of thin films and their annealing temperature. ZnO thin film has versatile structural as well as optical and electrical properties [9-10]. Due to excellent transmission and conductive features, it is a useful candidate for touch screens, optoelectronics devices, and display devices. ZnO thin films exhibit a major appearance in the II-VI semiconductor material [11]. ZnO is an n-type semiconductor material with a direct wide band gap energy (3.37 eV) and large exciton binding energy (60 meV) at room temperature [12]. ZnO has three different structures: Wurtzite, Zinc Blende, and Rock salt. Pure Zinc oxide has a hexagonal wurtzite crystal structure with lattice parameters such as  $a=3.248\text{\AA}$  and  $c=5.205\text{\AA}$  [13]. Thin films of ZnO were already synthesized by several methodologies such as spray pyrolysis [14], Pulsed Laser Deposition (PLD) [15], hydrothermal process [16], magnetron sputtering [17], dip coating [18], electron beam evaporation [19], spin coating and Sol-gel method [20-24]. In this study, ZnO thin film is formed by the Sol-gel spin coating method over the place of other methods due to their simplicity, cost-benefit, and easy availability. The properties of the prepared thin films are influenced by various properties such as annealing

\*Corresponding author E-mail: [Suman.rani@lpu.co.in](mailto:Suman.rani@lpu.co.in)

temperature [25], annealing time, layers or thickness, rotation of spin coater, the width of the thin film [26], and various substrates.

The optical transparency and electrical properties are greatly influenced by the thickness of the thin film and its annealing temperature. The thickness of thin films affects transmission due to the interference effect. The second major factor which affects the transparency and conductivity is heat treatment. They annually improve crystallinity, reduce defects, improve the adhesion with substrate, and affect the electrical properties. As far as we know, there hasn't been a detailed exploration in the existing literature that thoroughly examines how both annealing temperature and variations in thickness affect the optical and electrical properties of ZnO thin films. Therefore, it is crucial to optimize the annealing temperature and thickness of ZnO thin materials which are utilized in several applications of TCO materials. Colak et al. investigated the influence of ZnO thin films on the structure and electrical properties using the solid-state reaction method. Their conductivity ranges from  $8.7 \times 10^{-7}$  to  $3.1 \times 10^{-6} \Omega^{-1} \text{cm}^{-1}$  with a transmission of up to 80% [27]. Dahnoun et al. studied the influence of temperature on the structural, optical, and electrical properties of ZnO thin films, with conductivity ranging from 1.12 to  $2.86 \times 10^{-6} \Omega^{-1} \text{cm}^{-1}$  and 80% transmission [25]. In another study, Mansour et al. explored the optical and electrical properties of ZnO thin films, which showed 80% transmission and a conductivity of  $2.4 \times 10^{-7} \Omega^{-1} \text{cm}^{-1}$  [28]. Malek et al. focused solely on the electrical properties of ZnO thin films using a sol-gel dip-coating technique, with a conductivity value of  $4.07 \times 10^{-5} \Omega^{-1} \text{cm}^{-1}$  [29]. We are exploring an inventive notion: producing Zinc oxide thin films that possess dual attributes of excellent electrical conductivity and transparency. ZnO thin films are deposited on a Corning glass substrate by adopting the sol-gel spin coating method at various annealing temperatures, from 300°C to 500°C, at various layers thicknesses 189nm(S6), 237nm(S9), 253nm(S12), and 338nm(S15). Various characterization techniques were employed such as XRD, UV-visible spectroscopy, FE-SEM, and two-point techniques to study the structural, electrical, and optical properties of thin films.

## 2. Characterization Technique

The crystal structure and orientation of the thin film were examined by an X-ray diffractometer (Buker D8 Advance) with Cu-K $\alpha$  radiation at 1.5406 Å ranging from 20° to 60° by 0.02 increments. FE-SEM (FE-SEM: JEOLJSM-7610 F Plus) explained the thickness and surface morphology of the thin films while the chemical composition is confirmed by Energy Dispersive X-ray Analysis (EDX spectrum) (EDX-OXFORD EDX LN2 free). The optical properties of the thin films were carried out by UV-visible (Shimadzu) spectroscopy. The electrical properties were determined by the two-probe apparatus (SES-CAM TPX setup).

## 3. Synthesis Technique

To prepare thin films of ZnO, we employed the Sol-gel spin coating technique on the glass substrate. The thin films of ZnO were formed in two steps. In the first step, a clear and transparent sol was formed. The first materials utilized to prepare the sol are zinc acetate dehydrate (Zn(CH<sub>3</sub>COO)<sub>2</sub>·2H<sub>2</sub>O) as a precursor, 2-methoxy ethanol as a solvent, and mono ethanolamine as a sol stabilizer. Firstly, 0.5 M (5.5gm) of Zinc acetate dehydrate is dissolved in 50 ml of 2-methoxy ethanol. The solution is stirred between a temperature range of 50°C to 70°C for two hours to get a clear and homogeneous transparent solution. Lastly, 0.6ml of mono-ethanolamine is added after continuous stirring.

In the second step, thin films of solution are fabricated by performing the cleaning procedure of the glass substrate. For the formation of thin film, the cleaning process of the substrate played a major role in removing organic impurities. Firstly, the 2×2 cm glass substrates were cleaned with detergent followed by acetone and ethanol for 25 min by an ultrasonic cleaner (Bandelin Sonorex RK 100). Then finally cleaned with distilled water for 10 min and the glass substrates are dried properly. Prepared a clear and homogeneous transparent sol was deposited on a glass substrate for the formation of a thin film with the help of a programmable spin coater. After proper cleaning of the substrate, it is placed in the programmable spin coater where three uniform drops of prepared solution are placed in the middle of the substrate and then the substrate spins rapidly at the rate of 2000 rotations per minute. The film was preheated at 100°C for a few minutes. The same process has been repeated to obtain different numbers of layers such as 6, 9, 12, and 15, which are named S6(189nm), S9(237nm), S12(253nm), and S15(338nm). After the formation of various samples, the prepared thin films were placed in a furnace and subjected to post-heating for 5 hours at various temperatures ranging from 300°C to 500°C. Figure 1. shows preparation of ZnO thin films.

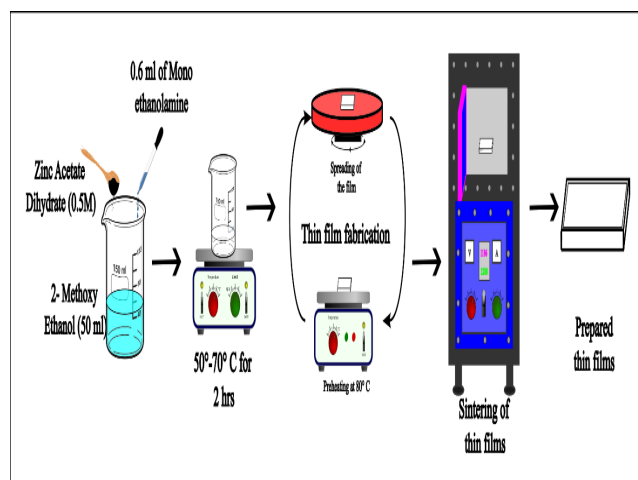


**Fig. 1:** Preparation of ZnO thin film by Sol-Gel spin coating method.

## 4. Results and Analysis

### 4.1 Structural Analysis

The phase structure and orientation of the ZnO thin films were analyzed by using an X-ray Diffraction pattern. Figure 2. exhibits the XRD pattern of 0.5M of Zinc Oxide thin films annealed at 300°C, 400°C, and 500°C for deposition of the thinnest, thin films of thickness 189nm(S6). The phase structure of prepared Zinc Oxide thin films is a hexagonal wurtzite structure with a strong (100) preferred orientation. Three major peaks (100), (002), and (101) were depicted at 500°C for S6 thin film. Diffraction peaks of ZnO thin films were compatible with JCPDS data 72-0163 with lattice parameters  $a=3.249\text{\AA}$  and  $c=5.20\text{\AA}$ . The XRD results show that the pure ZnO thin film phase structure was analyzed at 0.5 M concentration at 500°C deposited at six layers(S6) or thickness 189 nm and closely resembles the literature [30]. The structural parameters such as crystallite size (D), strain ( $\epsilon$ ) and dislocation density ( $\delta$ ) of ZnO thin films obtained from XRD data are represented in Table 1.

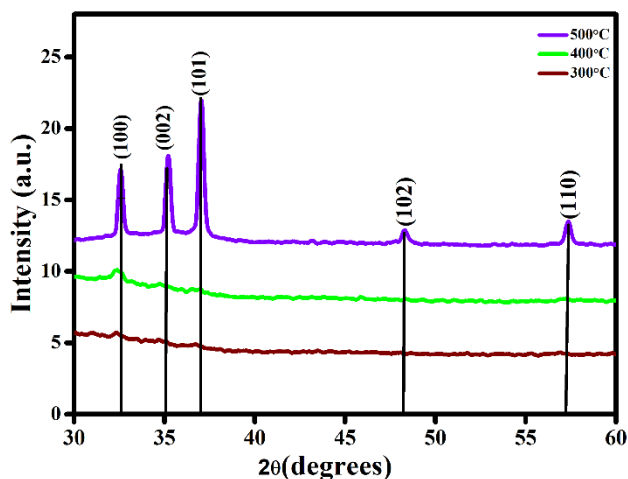


**Fig.2:** XRD spectra of six deposited layers (189nm thickness) of ZnO thin film annealed at 300°C, 400°C, 500°C

**Table 1:** Structural Properties of Six deposited layers (189nm) of ZnO thin film annealed at 300°C, 400°C, 500°C

Annealing Temperature (°C)	(2θ) (degrees)	(hkl)	FWHM(β) (degrees)	Crystallite size (D)(nm)	Strain (ε)(10 <sup>-3</sup> )	Dislocation Density δ)(10 <sup>-3</sup> )(nm <sup>-2</sup> )
300	32.31	100	0.57	14.51	2.4	4.8
400	32.39	100	0.54	15.32	2.3	4.3
500	32.56	100	0.29	28.54	1.2	1.2

In the X-ray Diffraction by using a Debye-Scherrer formula, we can evaluate the average crystallite size (D) of the material with the given equation (1)[31].

$$D = \frac{k\lambda}{\beta \cos\theta} \quad (1)$$

Where  $\lambda$  is the wavelength of the X-ray radiation utilized,  $2\theta$  is the highest angle of diffraction,  $\beta$  signifies Full Width Half Maximum (FWHM), and  $k$  represents the crystallite constant, and its value is 0.94. At the deposition of six layers S6(189nm) of ZnO annealed at 300°C,400°C 500°C, the FWHM value decreases with an increase in temperature and crystallite size increases, higher value of crystallite size (D) and a lower value of FWHM ( $\beta$ ) which expresses high crystallinity of the Zinc Oxide thin film. It can be observed that with the enhancement of annealing temperature, the crystallite size enhanced from 14.51 nm to 28.54 nm indicating better Crystallinity [32].

Dislocation density explains the size of defects in the crystallite. In XRD, it can be evaluated by the formula shown in the given equation (2)[33].

$$\delta = \frac{1}{D^2} \quad (2)$$

Table 1 indicates the value of dislocation density decreases due to increases in annealing temperature from 300°C to 500°C. The high value of crystallite size or the low value of dislocation density explains the better crystallinity of ZnO thin film [34].

The lattice strain of the ZnO thin films is evaluated by the formula shown in equation (3) [32].

$$\epsilon = \frac{\beta \cot\theta}{4} \quad (3)$$

The value of strain decreases with the enhancement of annealing temperature as shown in Table 1, which indicates that the value of lattice strain decreases due to the improvement of crystallinity [35]. Hence, the thinnest ZnO thin films S6 annealed at 300°C, 400°C, and 500°C temperatures show high crystallite size, less dislocation density, and low strain.

### 4.2 FE-SEM Analysis of ZnO thin films

The surface morphology, thickness, and particle size of the zinc oxide thin films were investigated by FE-SEM micrographs. In ZnO thin films concerning the annealing temperature, the thickness of 189nm remains the same due to the same deposition(S6). Figure 3 reveals the surface morphology and thickness of the thin films with various deposition layers. All the thin film shows good adhesion to the substrate. Images explained that particles are uniformly distributed over the glass substrate in all the layers. It is seen that thickness depends upon the deposition of layers. Fig.3 indicates that the SEM micrographs show crackles and homogeneous grain distribution [27]. In the SEM micrograph, particles are found in the range of 1µm and images were taken under the magnification of 25000. From the histogram, the average particle size has been analyzed by utilizing the ImageJ software shown in Figure 4. According to the analysis of FESEM particle size distribution, the estimated ZnO thin films particle size was calculated to be 96.28nm,94.27nm,92.46nm, and 85.21nm for S6, S9, S12, and S15 layers. The calculated average grain size decreases with the increment of the deposition

layer. It has been observed that thickness is enhanced and grain size decreases with the increase of deposition of layers. Hence the variation analyzed in the grain size of deposition of layers can be caused by the irregularity of organic group adsorption on ZnO crystallite surfaces [36].

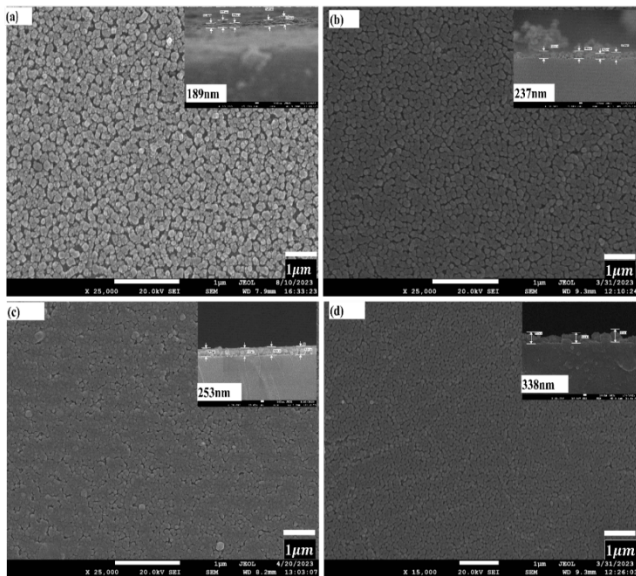


**Fig.3:** Surface morphology and cross-sectional micrographs of ZnO thin film at various deposition layers(thickness) S6(189nm), S9(237nm), S12(253nm), S15(338nm) annealed at 500°C at 45000 magnifications.

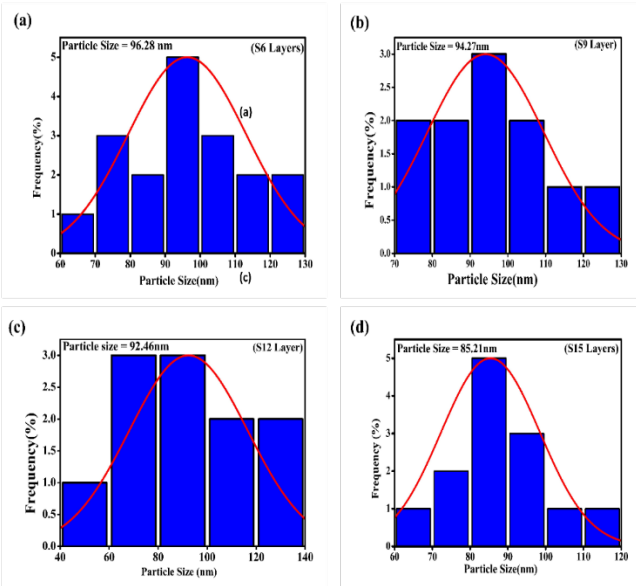


**Fig. 4:** Particle size of ZnO thin film at various deposition layers (thickness) such as S6(189nm), S9(237nm), S12(253nm), and S15(338nm).

#### 4.2.1 Compositional Analysis

Energy Dispersive spectroscopy (EDS) is a method that estimates the elemental composition of the material utilizing Scanning Electron Microscopes (SEM). Figure 5

depicts the presence of the elements in the material such as Zinc (Zn) and Oxygen (O). EDX spectra reveal that no impurity is present in it. It also shows the elemental mapping of the Zinc and oxygen with uniform propagation.

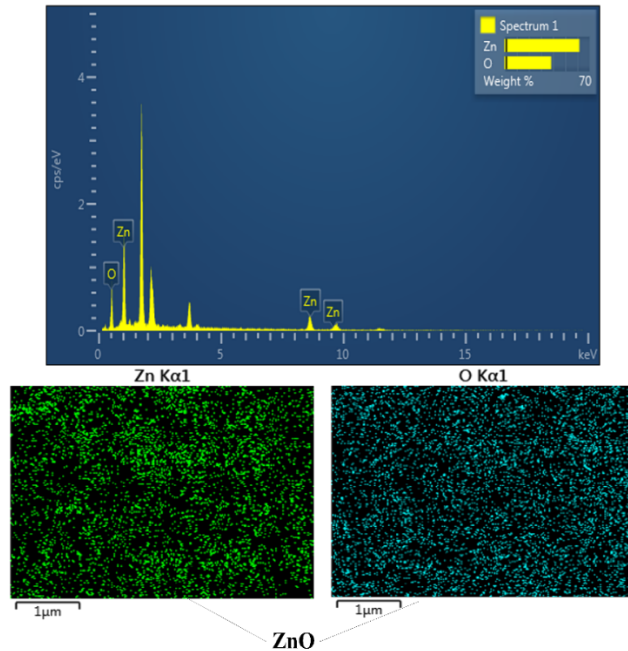


**Fig. 5:** EDX spectra and elemental mapping of Six depositions layers(189nm) of ZnO thin film annealed at 500°C.

#### 4.3. Optical Study of ZnO thin films

The material response in the presence of light is determined by its optical properties. Optical Properties are very crucial when related to the TCO material. Transmission, direct bandgap, extinction coefficient, absorption coefficient, and refractive index are the necessary parameters of TCO materials. Optical properties of ZnO thin films deposited on a glass substrate were studied by UV-visible spectroscopy concerning wavelength over the range of 300°C -500°C. Transmittance spectra of ZnO thin films concerning annealing temperature and thickness of thin film were shown in Figure 6(a) and 6(b) respectively. Figure 6(a) shows the annealing temperature importance, which significantly affects the transmittance. The % age of transmission increases with the increase of annealing temperature. At 300°C, the percentage of transmission is between (50 to 60) %, which is (60 to 70) % at 400°C. At 500°C, The maximum transmission achieved between (80 to 90) %. The increase in transmission concerning annealing temperature is attributed to the decreased number of defects or loss of light because of defect center dispersion. The decrease in defects indicates the improvement of crystal structure as explained in the XRD section. This finding indicates that ZnO thin film can be utilized as a transparent layer in several applications in the optoelectronics field such as display devices, photovoltaics, etc.

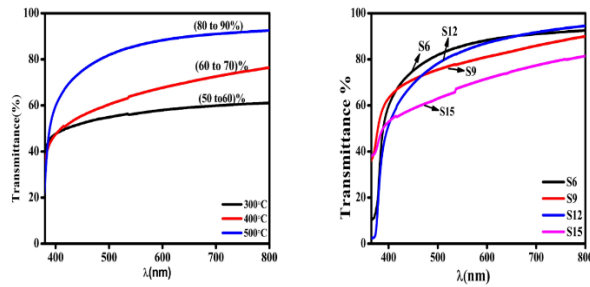


**Fig. 6:** UV-Visible spectra of ZnO thin films (a) concerning annealing temperatures such as 300°C, 400°C, 500°C (b) with respect to various thickness of thin films S6(189nm), S9(237nm), S12(253nm), S15(338nm) annealed at 500°C.

Understanding and utilizing the relation between thin film thickness and transmittance is vital for optimizing optical properties in various applications. It enables the design of coatings and devices that effectively control utilizing the transmitted light. In Figure 6(b), it was observed that transmittance decreases with the increase of thickness from 189nm to 338nm of ZnO thin film, and the maximum percentage of transmittance was achieved with S6 (189nm) thin film.

Absorption Coefficient ( $\alpha$ ) explains how far photons travel before being absorbed. The value of the absorption coefficient ( $\alpha$ ) is investigated by utilizing the data of absorption spectra in equation (4)

$$\alpha = \frac{2.303A}{t} \tag{4}$$

where ‘A’ is the absorption spectra, and ‘t’ is the thickness of the ZnO thin films which was observed through cross-sectional FESEM.

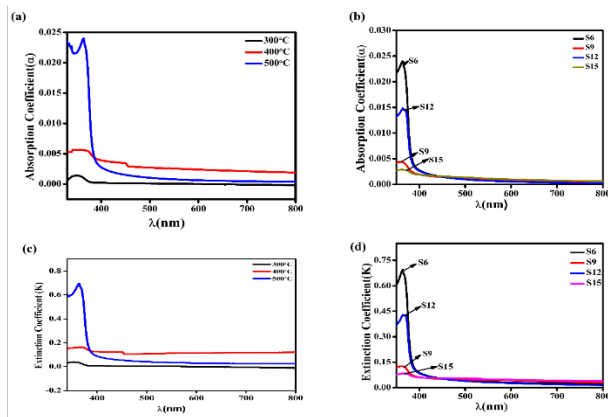


**Fig. 7:** UV-Visible absorption spectra of ZnO thin film (a) Absorption spectra concerning annealing temperature (b) Absorption spectra concerning various thicknesses of thin films annealed at 500°C. (c) Extinction coefficient of ZnO thin films concerning annealing temperature (d) concerning various thicknesses annealed at 500°C over the wavelength ranges from 400 to 800 nm.

Annealing temperature and deposition of layers (thickness) of ZnO thin film can significantly affect its UV

absorption properties. As shown in Fig.7(a,b), the absorption coefficient within the range of visible region has low values ( $\alpha < 3 \text{ cm}^{-1}$ ). In Figure 7(a), the value of the absorption coefficient increases with the increase of annealing temperature. At 500°C The material shows a maximum absorption coefficient. In Figure 7(b) the value of absorption coefficient decreases with the increase of thickness or deposition of layers (S6, S9, S12, S15). It shows that with the increase in thickness, the value of the absorption coefficient decreases. At the S6 layer(189nm) it shows maximum absorption coefficient. The order of absorption coefficient ( $\alpha$ ) in terms of thickness is  $S6 > S12 > S9 > S15$ .

The extinction Coefficient, also known as the attenuation coefficient (K), calculates how much energy is lost in electromagnetic radiation. The value of the extinction coefficient of ZnO thin film was investigated with the use of the absorption coefficient ( $\alpha$ ) in equation (5)[37].

$$k = \frac{\lambda\alpha}{4\pi} \tag{5}$$

Figure 7(c) indicates the increase in extinction coefficient values with the increase of annealing temperature from the ultraviolet region to the near visible region(320-360nm), which shows a slight absorption of ZnO thin film in the visible region. The annealed thin films show a lower value of extinction coefficient (about  $10^{-2}$ ) in the visible and near-infrared region, indicating a smooth surface of ZnO thin film. Figure 7(d) shows that with the increase of thickness, the extinction coefficient decreases from ultraviolet to near visible region(320-360nm). The order of extinction coefficient in terms of thickness for ZnO thin film is  $(S6 > S12 > S9 > S15)$ . The extinction coefficient depends upon the wavelength and property of the material.

To investigate the optical properties of a ZnO thin film, the refractive index is a necessary parameter which was calculated by equation (6)[38].

$$\eta = n + ik \tag{6}$$

where ‘n’ is the refractive index given by equation (7)[39]

$$n = 1 + \frac{\sqrt{R}}{1 - \sqrt{R}} \tag{7}$$

Where ‘R’ is the reflectance

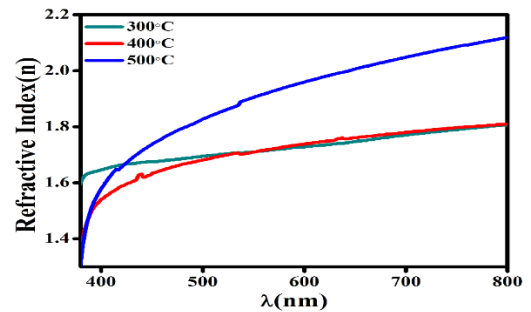


**Fig. 8:** Refractive Index of Zinc Oxide thin films deposition of 6 layers (S6) annealed at 300°C, 400°C, 500°C.

Figure 8 demonstrates the wavelength-dependent refractive index at various annealing temperatures (such as 300°C, 400°C and 500°C) of ZnO thin films (S6). Table 2 indicates that with the increase of the annealing temperature value, the refractive index also increases. The increasing tendency of refractive index within the wavelength ranging from 380 to 800 nm shows that the films have standard dispersion performance.

The absorption edge near the visible region is analyzed by the optical band gap. The optical band gap energy ( $E_g$ ) of ZnO thin film can be evaluated in the strong absorption region using the obtained data of absorption coefficient ( $\alpha$ ) from the Tauc's relation in equation 8 [40]

$$(\alpha h\nu)^m = C(h\nu - E_g) \quad (8)$$

Where 'C' is the constant of proportionality, 'h $\nu$ ' is the energy of the incident which can be evaluated by using the wavelength of UV-visible spectra 'E $_g$ ' is the optical band gap and  $\alpha$  is the absorption coefficient, and 'm' is the value of the exponent which depends on the transition type. For the direct band gap value of m is 2, the indirect band gap m is 1/2, the direct forbidden m is 2/3 and the indirect forbidden value of m is 1/3.

Figure 9. indicates the optical band gap of six deposition layers, 189nm of ZnO thin films annealed at various temperatures, such as 300°C, 400°C and 500°C. We found that the value of the optical band gap of ZnO thin films decreased from 3.98- 3.21 eV with increasing the annealing temperature from 300-500°C. In this study, the optical band gap was strongly dependent upon the annealing temperature. The decrease in optical band gap is due to two reasons; first (i) impurity concentration which brings narrowing effects, and second (ii) large crystalline sizes increase the bonding and antibonding and consequently band gap is decreased [41].

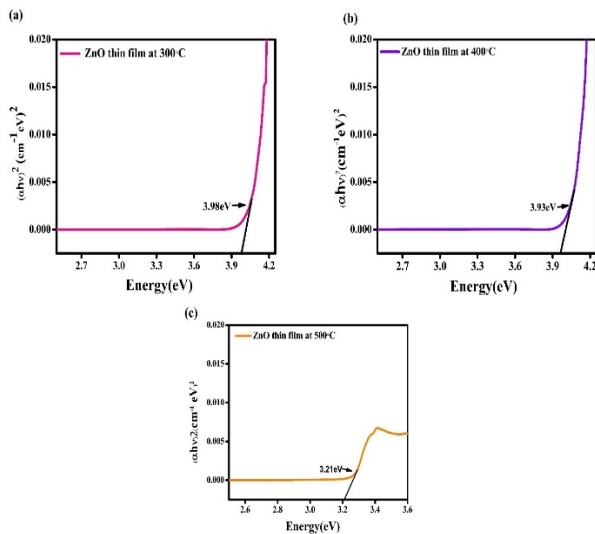


**Fig. 9:** Optical Band gap of six deposition layer (189nm) ZnO thin films annealed at 300°C, 400°C, 500°C.

**Table 2:** Refractive Index and optical band gap of Zinc Oxide thin films deposition of 6 layers (S6) annealed at 300°C, 400°C, 500°C.

Annealing Temperature (°C)	Refractive Index	Optical Bandgap (eV)
300°C	1.69	3.98
400°C	1.67	3.93
500°C	1.82	3.21

#### 4.4. Electrical Study of ZnO Thin Films

The Probe of two points, also called two-wire sensing, is commonly utilized for the characterization of semiconductor material [42]. It is often utilized to measure the resistivity of the thin films. The essential electrical property that distinguishes any material as a conductor, insulator, or semiconductor is its electrical resistivity ( $\rho$ ). For the exploration of new materials for electronic applications, electrical resistivity ( $\rho$ ) constitutes a crucial property that is evaluated or quantified [43].

One of the easiest and most efficient methods for determining the I-V of a thin film is to use a two-point probe setup, in which each contact serves as both a voltage (V) probe source and a current (I) probe source. SES-CAMM two probe instrument, TPX set up was used for this research. To confirm the ohmic connection of the thin film, a silver paste has been utilized. Evaluations were done on the resistivity and conductivity values of ZnO thin films at various annealing temperatures 300°C, 400°C, 500°C and various layers of thickness S6(189nm), S 9(237nm), S12(253nm) and S15(338nm). The value of resistivity ( $\rho$ ) is evaluated by using the relation in equation (9) [44].

$$\rho = \frac{\pi t}{\ln 2} \left( \frac{V}{I} \right) = 4.532 \left( \frac{V}{I} \right) \quad (9)$$

where 'V' represents the applied voltage, 'I' represents the current, and 't' represents the thickness of the Zinc Oxide thin films. 'Rs' represents the sheet resistance of the thin film which is electrical resistance per unit square. The value of sheet resistance was analyzed by calculating the slope of the Voltage applied versus the Current obtained by two-probe data. Thus, the value of sheet resistance ( $R_s$ ) for ZnO thin film concerning annealing temperature and layers or thickness was calculated by using two probe instruments explained in equation (10).

$$R_s = 4.532 \frac{V}{I} \quad (10)$$

$$\rho = R_s \times t \quad (11)$$

The value of electrical resistivity ( $\rho$ ) explained in equation (11) was used to get the value of electrical conductivity ( $\sigma$ ) which is the reciprocal of electrical resistivity ( $\rho$ ) given in equation (12)

$$\sigma = \frac{1}{\rho} \quad (12)$$

Figure 10 (a,b) shows the graph of voltage versus current of ZnO thin film concerning annealing temperature and layers

or thickness. All the samples show smooth and ohmic behavior, which depicts that ZnO thin films are semiconductors in nature. An increase in electrode voltage correspondingly increases the current flowing through the thin film. In Figure 10(a,b), it was observed that an increment in forward current at all voltages implies that the thin films have higher conductivity. This increased forward current may contribute to higher solar cell manufacturing efficiency [45].

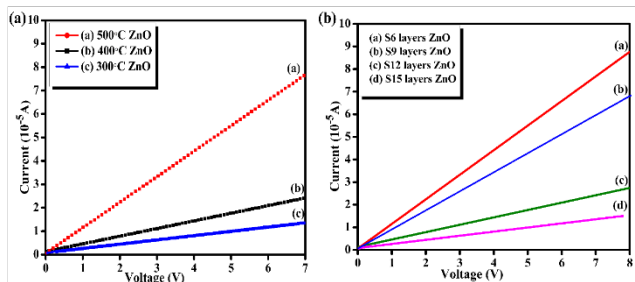


**Fig. 10:** a) IV Graph of Zinc Oxide thin films annealed at 300°C,400°C and 500°C.b) IV graph of Zinc Oxide thin film at various layers S6, S9, S12, S15.

Figure 11. (a,b) explains the electrical conductivity and transmission(%) of ZnO at various annealing temperatures and various numbers of layers (thickness). Fig.11(a) depicts the variation of conductivity. It was observed that with the increase of annealing temperature, the value of conductivity increases. Table 3 presents the values of electrical conductivity and transmission (%) of ZnO thin film annealed at 300°C,400°C and 500°C. It was analyzed that the increase in conductivity is due to the increase in heat treatment of thin films. The electrical conductivity of ZnO thin film is regulated by the defects produced at high temperatures [46]. Figure 11 (b) shows a decrease in conductivity with the increase in number of layers (thickness). In Table 4. The value of conductivity decreases with the increase of layers or thickness from S6(189nm) to S12(338nm). films exhibit a decrease in electrical conductivity due to the variation in thickness [47]. Hence, it predicts that ZnO thin film will be a better candidate for Transparent conducting oxide (TCO) at 500°C with 189nm thickness (or six layers of deposition).

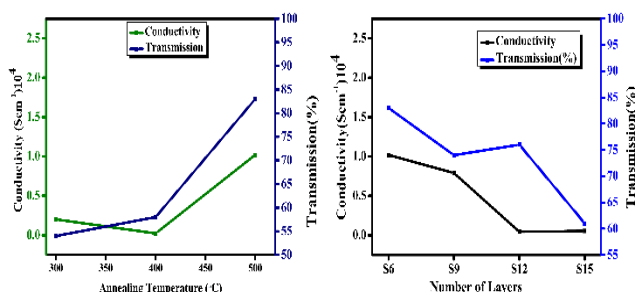


**Fig. 11:** Electrical Conductivity plot (a) concerning the annealing temperature such as 300°C ,400°C 500°C (b) with respect to Layers such as S6(189nm) ,S9(237nm),S12(253nm),S15(338nm).

**Table 3:** Electrical Conductivity and transmission of ZnO thin film annealed at 300°C,400°C,500°C.

Annealing Temperature (°C)	Conductivity $\sigma(\text{Scm}^{-1}) 10^4$	Transmission (%)
300°C	0.02	54
400°C	0.23	58
500°C	1.02	83

**Table 4:** Electrical Conductivity and transmission of ZnO thin film at various layers S6, S9, S12, S15 annealed at 500°C.

No. of Layers (S)	Conductivity $\sigma(\text{S/cm}^{-1}) 10^4$	Transmission (%)
S6	1.02	83
S9	0.79	74
S12	0.44	76
S15	0.54	61

#### 4.4.1. Activation Energy

Activation energy is the minimal energy required to excite or activate molecules or atoms so that they can go through transformation. Since electrical conductivity in semiconductors is a thermally generated process, it commonly rises exponentially with temperature. It depends upon the deposition temperature. Hence, the relation between the deposition temperature, conductivity, and activation energy of the thin film is based on Arrhenius Law given in the equation (13)

$$\sigma = \sigma_0 \exp\left(-\frac{\Delta E_a}{KT}\right) \tag{13}$$

where  $\sigma$  represents electrical conductivity,  $\Delta E_a$  represents the activation energy of the thin film,  $\sigma_0$  known as conductivity at absolute temperature,  $K$  represents Boltzmann constant, and  $T$  is the absolute temperature [48]. From equation (13) values of activation energy were determined by the Slope of the linear part of the  $\log\sigma$  versus  $1000/T$  curve (Figure12). Based on the semiconductor's conduction process, the Arrhenius equation can be expanded to equation (14)

$$\sigma = \sigma_1 \exp\left(-\frac{E_{a1}}{KT}\right) + \sigma_2 \exp\left(-\frac{E_{a2}}{KT}\right) \tag{14}$$

where the activation energies for the two conduction areas are represented by  $E_{a1}$  and  $E_{a2}$ . A sample of ZnO thin film at various annealing temperatures was chosen because the thin films comparatively improved substrate adherence. Figure 12 indicates two straight lines that signify the two terms ( $E_{a1}$  and  $E_{a2}$ ). These terms show two distinct mechanisms of conductivity of ZnO thin film between the temperatures. The slope of the  $\log\sigma$  versus  $1000/T$  of these lines gives the value of the estimated activation energies of the area. Table5. illustrate that the activation energy for all samples is less in the first region and high in the second region due to the material moving from one conduction mechanism to another. In the area of high temperature, it is higher than the low-temperature region. In the region of high temperature, the conductivity is analyzed by intrinsic defects, which is known as intrinsic conduction. The high

activation energy in the first region might be explained by the fact that the energy required to form the defects is much more than the energy required for its drift. Due to this reason, the electrical conductivity of the samples at high temperatures is determined by intrinsic facts that are caused by thermal fluctuations [49]. Also with the increase of annealing temperature of ZnO thin films from 300°C to 500°C, the value of activation energy increases from  $E_{a1}=0.091\text{eV}$ ,  $E_{a2}=0.78$  to  $E_{a1}=0.57\text{eV}$ ,  $E_{a2}=0.865\text{eV}$ .

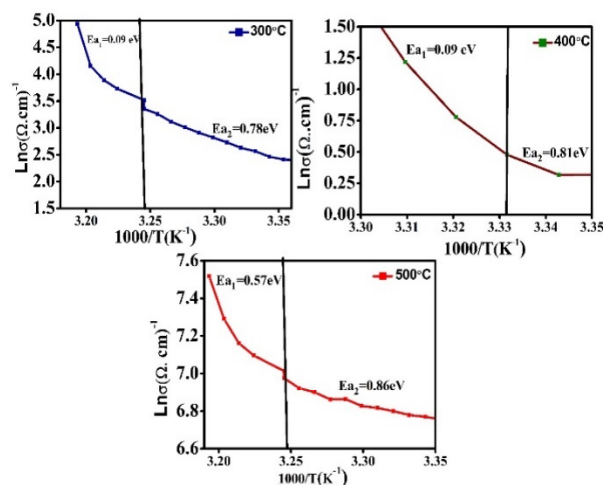


**Fig. 12:** Activation Energy plot of six deposition layers (189nm) of ZnO thin films annealed at 300°C, 400°C, 500°C.

**Table 1:** The activation energy of S6 (189nm) of ZnO thin films annealed at 300°C, 400°C, and 500°C.

Annealing temperature (°C)	Activation energy ( $E_{a1}$ ) (eV)	Activation energy ( $E_{a2}$ ) (eV)
300	0.09	0.78
400	0.26	0.81
500	0.57	0.87

#### 4.4.2. Figure of Merit

The quality and performance of any transparent conducting oxide are determined by using a parameter known as the Figure of Merit (FOM). When the electrical sheet resistance and optical transmittance of transparent conducting oxides are known, FOM is a necessary tool for comparing their performance [50]. Hacke defined the concept of the Figure of Merit [51]. The value of FOM is evaluated by using the relation in equation (15)

$$\text{FOM} = \frac{T_{\text{av}}}{R_s} \quad (15)$$

Where  $T_{\text{av}}$  represents the average transmission in the visible range (400-800nm) and  $R_s$  represents the sheet resistance of the ZnO thin film. A higher value of the Figure of merit signifies the superior quality of the thin film. Figure 13. (a) shows a graph of the Figure of merit versus annealing temperature of ZnO thin film. The value of the Figure of merit increases with the increase of annealing temperature. It shows that 500°C is the best annealing temperature for

transparent conducting oxides (TCO) where the material depicts better conductivity and transparency than another temperature. Figure 13. (b) shows a plot of the Figure of merit versus a number of layers (thickness) of the ZnO thin Film. In this graph, the value of the Figure of merit decreases with the increase of a number of layers or thickness. It shows that 189nm is the best candidate for Transparent conducting oxides among the other layers. Thus, the Figure of merit (FOM) suggests that the ZnO film will behave better at 500°C with 189nm thickness, supporting its use as an affordable Transparent conducting oxide film in optoelectronic devices.

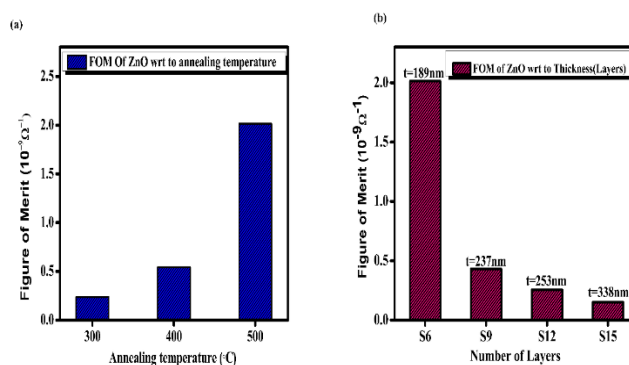


**Fig. 13:** (a) Figure of merit of ZnO thin films (a) annealed at 300°C, 400°C, 500°C (b) various deposition layers (thickness) S6 (189nm), S9 (237nm), S12 (253nm), S15 (338nm) annealed at 500°C.

## 5. Conclusion

In the present study, we prepared Zinc Oxide thin films by sol-gel spin coating method and analyzed the influence of annealing temperature and thickness on the structural, optical, and electrical properties. The optical transparency and electrical properties are greatly affected by the thickness of thin films and their annealing temperature. It indicates that with the enhancement of annealing temperature, crystallite size increases, strain decreases, and dislocation density decreases. 189nm of ZnO thin film annealed at 500°C shows the best crystallinity among other samples. FE-SEM shows homogeneous and crackless thin films at a thickness of 189 nm, and investigated that with the increase of several layers (S6 to S15), the thickness increases from 189nm to 338nm. At 500°C of ZnO thin film thickness up to 189nm shows 83% transmission in the range of visible spectra. According to the optical study, a 189nm thin film annealed at 500°C shows better performance among all samples. material. At 500°C and 189nm thickness, the value of conductivity and activation energy is  $1.02 \times 10^4 (\text{Scm}^{-1})$  and  $E_{a1}=0.570\text{eV}$ ,  $E_{a2}=0.865\text{eV}$ . Hence, the figure of merit shows the material's better transparency and electrical conductivity. So, it suggests that the ZnO film will behave better at 500°C with 189nm thickness for optoelectronics devices such as solar cells, display devices, and photovoltaic devices.



**Acknowledgments:**

For providing the characterization facility, the authors are grateful to Central Instrumentation Facility, Lovely Professional University-Punjab, India.

**Author contribution:**

All authors contributed to the conceptualization and design of the study. Shruti Bakshi managed material preparation, and data collection, and authored the initial draft. Suman Rani assisted in the result analysis and reviewed the final manuscript draft. All authors read and approved the final manuscript.

**Funding:**

The authors declare that no funds, grants, or other support were received during the preparation of this manuscript.

**Conflict of interest:**

The authors declared that they have no conflict of interest.

**References**

- [1] Thakur, Y. S., Acharya, A. D., & Sharma, S. (2023). Reinforcement of V<sub>2</sub>O<sub>5</sub> nanoparticle in polyaniline to improve the optical and UV-shielding properties. *Results in Optics*, *11*, 100400.
- [2] Kumar, P., Nisha, Sarkar, P., Singh, S., Mishra, B.C.K., Katiyar, R.S.: The influence of post-growth heat treatment on the optical properties of pulsed laser deposited ZnO thin films. *Appl. Phys. A*, *128*, 372 (2022).
- [3] Muchuweni, E., Sathiaraj, T. S., Nyakoty, H.: Effect of gallium doping on the structural, optical and electrical properties of zinc oxide thin films prepared by spray pyrolysis. *Ceram. Int.* **42**, 10066-10070(2016).
- [4] Muchuweni, E., Sathiaraj, T.S., Nyakoty., H.: Low temperature synthesis of radio frequency magnetron sputtered gallium and aluminium co-doped zinc oxide thin films for transparent electrode fabrication. *Appl. Surf. Sci.* **390**, 570-577(2016).
- [5] Lee, J.H., Ko, K.H, Park, B.O.: Electrical and optical properties of ZnO transparent conducting films by the sol-gel method. *J. Cryst. Growth*, **247**, 119-125(2003).
- [6] Sathiaraj, T.S.: Effect of annealing on the structural, optical and electrical properties of ITO films by RF sputtering under low vacuum level. *Microelectron. J.* **39**, 1444-1451(2008).
- [7] Srivastava, A.K., Kumar, J.: Effect of zinc addition and vacuum annealing time on the properties of spin-coated low-cost transparent conducting 1 at% Ga-ZnO thin films. *Sci.Tech.Adv.Mater.* **14**, 065002(2013).
- [8] Muchuweni, E., Sathiaraj, T.S., Nyakoty, H.: Physical properties of gallium and aluminium co-doped zinc oxide thin films deposited at different radio frequency magnetron sputtering power. *Ceramics International*, **42**,17706-17710(2016).
- [9] Jun, M.C., Koh, J.H.: Optical and structural properties of Al-doped ZnO thin films by sol-gel process. *J. Nanosci. Nanotechnol.* **13**, 3403-3407(2013).
- [10] Kaźmierczak-Bałała, A., Bodzenta, J., Guzewicz, M.: Microscopic investigations of morphology and thermal properties of ZnO thin films grown by atomic layer deposition method. *Ultramicroscopy*, **210**, 112923(2020).
- [11] Nagayasamy, N., Gandhimathination, S., Veerasamy, V.: The effect of ZnO thin film and its structural and optical properties prepared by sol-gel spin coating method. *Open.J.Metal.* (2013).
- [12] Abd Halim, A.A., Hashim, H., Rusop, M., Mamat, M.H., Zoolfakar, A.S.: Study on electrical properties of Zinc Oxide thin film. *IEEE. Conf. Innov. Technol. Intell. Syst. Indust. Appl.* 123-126, (2008).
- [13] Yousif, A.A., Habubi, N.F., Haidar, A.A.: Nanostructure zinc oxide with cobalt dopant by PLD for gas sensor applications. *J. Nano. Elect. Phys.* **4**,02007 (2012).
- [14] Özdoğan, M., Çelebi, C., Utlu, G.: Mechanisms behind slow photoresponse character of Pulsed Electron Deposited ZnO thin films. *Mater. Sci. Semi. Process.*, **107**, 104863 (2020).
- [15] Saleem, M., Fang, L., Ruan, H.B., Wu, F., Huang, Q.L., Xu, C.L., Kong, C.Y.: Effect of zinc acetate concentration on the structural and optical properties of ZnO thin films deposited by Sol-Gel method. *Int. J. Phys. Sci.* **7**,2971-2979 (2012).
- [16] Gumus, C.E.B.R.A.İ.L., Ozkendir, O.M., Kavak, H., Ufuktepe, Y.Ü.K.S.E.L.: Structural and optical properties of zinc oxide thin films prepared by spray pyrolysis method. *J.Optolect. Adv.Mater.* **8**, 299-303 (2006).
- [17] Hasabeldaim, E.H.H., Ntwaeaborwa, O.M., Kroon, R.E., Coetsee, E., Swart, H.C.: Luminescence properties of Eu doped ZnO PLD thin films: The effect of oxygen partial pressure. *Superlatt. Microstruct.* **139**, 106432 (2020).
- [18] Akhavan, O., Mehrabian, M., Mirabbaszadeh, K. and Azimirad, R.: Hydrothermal synthesis of ZnO nanorod arrays for photocatalytic inactivation of bacteria. *J. Phys. Appl. Phys.* **42**, 225305 (2009).
- [19] Abdullahi, S., Momoh, M., Yahya, H.N.: Influence of nitrogen annealing on the structural and electrical properties of zinc oxide (ZnO) thin film deposited by

- radio frequency magnetron sputtering technique. *IOSR. Env. Sci. Tox. Food. Technol.* **4**,81-85 (2013)
- [20] Kaneva, N.V., Dushkin, C.D.: Preparation of nanocrystalline thin films of ZnO by sol-gel dip coating. *Bulg. Chem. Commun.* **43**, 259-263 (2011).
- [21] Agarwal, D.C., Chauhan, R.S., Kumar, A., Kabiraj, D., Singh, F., Khan, S.A., Avasthi, D.K., Pivin, J.C., Kumar, M., Ghatak, J., Satyam, P.V.: Synthesis and characterization of ZnO thin film grown by electron beam evaporation. *J. Appl. Phys.*, **99**,123105 (2006).
- [22] Yahia, S.B., Znaidi, L., Kanaev, A., Petitet, J.P.: Raman study of oriented ZnO thin films deposited by sol-gel method. *Spectrochimica Acta Part A: Mol. Biomol. Spectro.*, **71**,1234-1238 (2008).
- [23] Singh, A., Kumar, A., Suri, N., Kumar, S., Kumar, M., Khanna, P.K. and Kumar, D., 2009. Structural and optical characterization of ZnO thin films deposited by sol-gel method. *J. Optoelect. Advanc. Mater.* **11**, 790 (2009).
- [24] Li, H., Wang, J., Liu, H., Yang, C., Xu, H., Li, X., Cui, H.: Sol-gel preparation of transparent zinc oxide films with highly preferential crystal orientation. *Vacuum.* **77**, 57-62 (2004).
- [25] S,Ilcan., S., Caglar, Y., Caglar, M., Preparation and characterization of ZnO thin films deposited by sol-gel spin coating method. *J. Optoelectron. Advanc. Mater.*, **10**,2578-2583 (2008).
- [26] Shikha, D., Mehta, V., Sood, S.C. and Sharma, J., Structural and optical properties of ZnO thin films deposited by sol-gel method: effect of stabilizer concentration. *J. Mater. Sci. Mater. Electron.* **26**,4902-4907 (2015).
- [27] Dahnoun, M., Attaf, A., Saidi, H., Yahia, A., Khelifi, C.: Structural, optical and electrical properties of zinc oxide thin films deposited by sol-gel spin coating technique. *Optik.* **134**, 53-59 (2017).
- [28] Benramache, S., Aoun, Y., Lakel, S., Benhaoua, B.: The effect of film thickness on the structural, optical and electrical properties of ZnO thin films deposited by ultrasonic spray deposition. *Mater. Research. Exp.* **6**, 26418 (2019).
- [29] Çolak, H.: Influence of Tm<sub>2</sub>O<sub>3</sub> doping on structural and electrical properties of ZnO. *J. Mater. Sci. Mater. Electron.* **26**,784-790 (2015).
- [30] Mansour, S. A., & Yakuphanoglu, F. (2012). Electrical-optical properties of nanofiber ZnO film grown by sol gel method and fabrication of ZnO/p-Si heterojunction. *Solid State Sciences*, *14*(1), 121-126
- [31] Malek, M. F., Zakaria, N., Sahdan, M. Z., Mamat, M. H., Khusaimi, Z., & Rusop, M. (2010, April). Electrical properties of ZnO thin films prepared by sol-gel technique. In *2010 International Conference on Electronic Devices, Systems and Applications* (pp. 384-387). IEEE.
- [32] Nagayasamy, N., Gandhimathination, S., Veerasamy, V.: The effect of ZnO thin film and its structural and optical properties prepared by sol-gel spin coating method. *Open. J. Metal.* **3**,8-11 (2013).
- [33] Benramache, S., Rahal, A., Benhaoua, B.: The effects of solvent nature on spray-deposited ZnO thin film prepared from Zn (CH<sub>3</sub>COO)<sub>2</sub> · 2H<sub>2</sub>O. *Optik.* **125**, 663-666 (2014).
- [34] Herissi, L., Hadjeris, L., Moualkia, H., Abdelmalek, N., Attaf, N., Aida, M.S., Bougdira, J.: Realization and study of ZnO thin films intended for optoelectronic applications. *New Technol. Mater.* **1**,39-43 (2011)
- [35] Bala, A., Rani, S.: UV excited emission spectra of gadolinium aluminium garnet. *J. Opt.* **52**, 868-874 (2023)
- [36] Sadananda Kumar, N., Bangera, K.V., Shivakumar, G.K.: Effect of annealing on the properties of zinc oxide nanofiber thin films grown by spray pyrolysis technique. *Appl. Nanosci.* **4**, 209-216(2014).
- [37] Bala, A., Rani, S.: Down conversation visible emission spectra of Cr<sup>3+</sup> doped gadolinium aluminum garnet. *Opt. Quant. Electron.*, **55**,866 (2023)
- [38] Aryanto, D., Hastuti, E., Taspika, M., Anam, K., Isnaeni, I., Widayatno, W.B., Wismogroho, A.S., Marwoto, P., Nuryadin, B.W., Noviyanto, A., Sugianto, S.: Characteristics and photocatalytic activity of highly c-axis-oriented ZnO thin films. *J. Sol-Gel. Sci. Technol.* **96**, 226-235 (2020).
- [39] Pudukudy, M., Yaakob, Z.: Facile synthesis of quasi spherical ZnO nanoparticles with excellent photocatalytic activity. *J. Cluster Sci.* **26**,1187-1201 (2015).
- [40] Sanjeev, S., Kekuda, D.: Effect of annealing temperature on the structural and optical properties of zinc oxide (ZnO) thin films prepared by spin coating process. *Mater. Sci. Engineer.* **73**,012149 (2015).
- [41] Tauc, J.: Band tails in amorphous semiconductors. *J. Non-Crystall. Solids.*, **97**,149-154 (1987).
- [42] Jalil, Z.: Structural and optical properties of zinc oxide (ZnO) based thin films deposited by sol-gel spin coating method. *J. Phys.* **1116**, 032020 (2018).
- [43] Chandra, N., Sharma, V., Chung, G.Y., Schroder, D.K.: Four-point probe characterization of 4H silicon carbide. *Solid-state. Electron.* **64** 73-77 (2011).
- [44] Barquinha, P.M.C.: Transparent oxide thin-film transistors: production, characterization and

- integration (Doctoral dissertation, Universidade NOVA de Lisboa (Portugal) (2010).
- [45] Emegha, J.O., Olofinjana, B., Ukhurebor, K.E., Adegbite, J.T., Eleruja, M.A.: Electrical properties of semiconducting copper zinc sulphide thin films. *Current. Appl. Sci. Technol.* 22, 10-55003 (2022)
- [46] Thirumavalavan, S., Mani, K., Sagadevan, S.: Investigation of the structural, optical and electrical properties of copper selenide thin films. *Mater. Res.* 18 1000-1007 (2015).
- [47] Çolak, H., Türkoğlu, O.: Structural and electrical properties of V-doped ZnO prepared by the solid state reaction. *J. Mater. Sci. Mater. Electron.* , 23, 1750-1758 (2012).
- [48] Rao, T.P. and Santhoshkumar, M.C., 2009. Effect of thickness on structural, optical and electrical properties of nanostructured ZnO thin films by spray pyrolysis. *Appl. Surf. Sci.* 255,4579-4584 (2009).
- [49] Deshpande, V.P., Sartale, S.D., Vyas, A.N., Ubale, A.U.: Temperature dependent properties of spray deposited nanostructured ZnO thin films. *Int. J. Mater. Chem.*, 7, 36-46 (2017).
- [50] Patil, A.V., Dighavkar, C.G., Sonawane, S.K., Patil, S.J., Borse, R.Y.: Effect of firing temperature on electrical and structural characteristics of screen printed ZnO thick films. *J. Optoelectron. Biomed. Mater.* 1, 226-233 (2009).
- [51] Tonny, K.N., Rafique, R., Sharmin, A., Bashar, M.S., Mahmood, Z.H.: Electrical, optical and structural properties of transparent conducting Al doped ZnO (AZO) deposited by sol-gel spin coating. *AIP. Advan.*, 8, 065307 (2018).